AIP | Journal of Applied Physics

Impact of nonpolar AlGaN quantum wells on deep ultraviolet laser diodes

K. Kojima, A. A. Yamaguchi, M. Funato, Y. Kawakami, and S. Noda

Citation: J. Appl. Phys. **110**, 043115 (2011); doi: 10.1063/1.3627180
View online: http://dx.doi.org/10.1063/1.3627180
View Table of Contents: http://jap.aip.org/resource/1/JAPIAU/v110/i4
Published by the American Institute of Physics.

Impact of nonpolar AlGaN quantum wells on deep ultraviolet laser diodes

K. Kojima,[1,a)] A. A. Yamaguchi,[2] M. Funato,[1] Y. Kawakami,[1] and S. Noda[1]
[1]*Department of Electronic Science and Engineering, Kyoto University, Kyoto 615-8510, Japan*
[2]*Optoelectronic Device System R&D Center, Kanazawa Institute of Technology, Ishikawa 921-8501, Japan*

(Received 4 April 2011; accepted 21 July 2011; published online 31 August 2011)

The radiation properties of nonpolar AlGaN quantum wells (QWs) were theoretically investigated by comparing them to those of *c*-plane AlGaN QWs with heavy holes as the top valence band (VB). First, the conditions to minimize the threshold carrier density of *c*-plane QW laser diodes were explored. A thin well width (~1 nm) and reduction of the Al content in the well layer were important to reduce threshold carrier density because narrow wells suppressed the quantum confined Stark effect and AlGaN with a lower Al content had a lower density of states. Moreover, the emission wavelength was widely controlled by tuning the Al contents of both the well and barrier layers under the proposed conditions. Then the properties of nonpolar AlGaN QWs were investigated. Nonpolar AlGaN had several superior characteristics compared to *c*-plane QWs, including large overlap integrals, optical polarization suitable for both edge and surface emissions, an almost linearly polarized optical dipole between the conduction band and top VB due to the isolated VBs, and a reduced VB density of state. Finally, the threshold carrier densities of both nonpolar and optimized *c*-plane QWs were compared as functions of the transition wavelength. At a given wavelength, the threshold of nonpolar QWs was lower than that of *c*-plane ones. Particularly below 260 nm, nonpolar QWs had a low threshold, whereas that of *c*-plane QWs drastically increased due to the large VB mass of AlN and carrier population in the crystal-field splitting band. © *2011 American Institute of Physics*. [doi:10.1063/1.3627180]

I. INTRODUCTION

Recently, AlGaN related deep ultraviolet (DUV) emitters have been intensively investigated to replace mercury lamps as well as to realize small and efficient sanitary light sources with high photon energies.[1–4] AlGaN also displays a unique optical polarization anisotropy phenomenon.[5–7] Therefore, AlGaN semiconductors are attractive in both applied and basic physics. However, the external and wall-plug efficiencies of AlGaN light emitting diodes (LEDs) remain very low, and the threshold of AlGaN laser diodes (LDs) are currently very large. In particular, lasing with current injection for LDs occurs in a limited wavelength regime.[8]

To expand the lasing wavelength of AlGaN LDs, we propose crystal growth along non-*c*-plane directions. Some studies have grown nonpolar AlGaN quantum wells (QWs), while others have theoretically investigated the fundamental electronic properties of non-*c*-plane AlGaN QWs.[9,10] In this study, we theoretically investigate the optical characteristics of nonpolar AlGaN QWs to elucidate the differences between the *c*-plane and nonpolar plane QWs, especially for use as emitting layers in LD devices.

II. THEORIES AND MODELS

Valence band (VB) structures are computed by $\mathbf{k}\cdot\mathbf{p}$ perturbation techniques.[11,12] To consider the quantum confined Stark effect (QCSE) suppression due to field screening by excited carriers, self-consistent computation is performed by coupling Schrödinger and Poisson equations. Then the optical gain is numerically calculated based on the band structure. The sample structure in this study is $Al_xGa_{1-x}N/Al_yGa_{1-y}N$, where $Al_xGa_{1-x}N$ and $Al_yGa_{1-y}N$ represent the emitter (well) and barrier layers, respectively. The emitter layers are assumed to be fully coherent to the barrier layer material, which has a native lattice constant. Except for the crystal-field splitting-energy Δ_{cr} of −217 meV,[13] the material parameters are from a conventional report.[14] For the deformation potentials of GaN, we also referred to Ref. 15 and compared these potentials to the conventional parameters. The terms transverse-electric (TE) field and transverse-magnetic (TM) field represent light where the dominant polarization is parallel and perpendicular to the growth surface, respectively. TE and TM are independent of growth orientation.

III. BAND STRUCTURE OF *C*-PLANE AND NONPOLAR ALGAN SYSTEMS

Figure 1(a) shows the top VB of an $Al_xGa_{1-x}N/Al_yGa_{1-y}N$ heterostructure on the *c*-plane. When the emitter Al content x is zero, the emitter represents GaN and the top VB, which dominates the radiation properties of the emitter, represents a heavy hole (HH). However, when x increases, the VB energy of crystal-field-splitting hole (CH) overcomes that of HH, and CH becomes the top VB because Δ_{cr} of AlN has a large negative value. The boundary between the HH-top and CH-top is illustrated in Fig. 1 as white solid line, and the line is roughly given by $x \sim 0.6y$. Considering quantum confinement in a QW structure, the crossover Al content depends on the quantum well width due to the vertical mass

a)Author to whom correspondence should be addressed. Electronic mail: kkojima@qoe.kuee.kyoto-u.ac.jp.

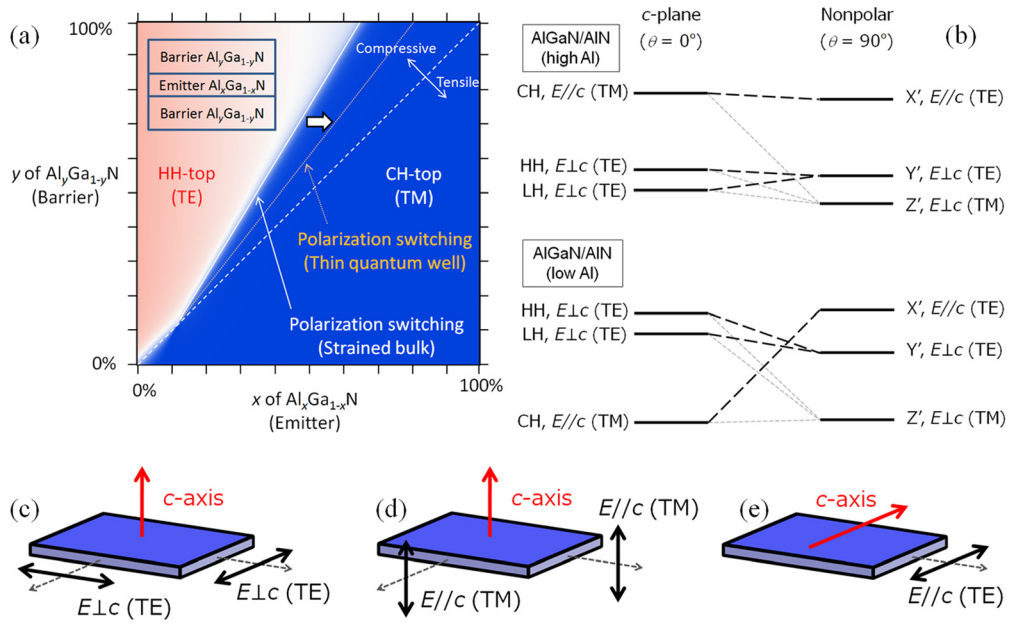

FIG. 1. (Color online) (a) Diagram of the top VB of a *c*-plane $Al_xGa_{1-x}N$/ $Al_yGa_{1-y}N$ heterostructure. (b) VB line-up of AlGaN/AlN on the *c*-plane and nonpolar plane. Possible geometries of LD cavities for (c) *c*-plane AlGaN/AlN with a low Al content, (d) *c*-plane AlGaN/AlN with a high Al content, and (e) nonpolar AlGaN/AlN (x' polarization) where red solid, black solid, and black dashed arrows represent the *c*-axis, electric-field, and propagation direction of light, respectively.

difference between HH and CH.[7,16] Thus, the quantum effect modifies the crossover line, and the condition is approximately given by $x \sim 0.8y$ when the well width is thin. In this article, we only consider the situation where $x < y$ ($Al_xGa_{1-x}N$ is compressively strained on $Al_yGa_{1-y}N$) to confine the carriers in the emitter layer using the QW structure.

When CH is the top VB of the emitter layer, CH has difficulty confining carriers even with the use of QW structures. For example, the overlap integrals between electrons and CH wave functions in a 1-nm-thick $Al_{0.9}Ga_{0.1}N$/AlN single QW is 1.6%, but is 48% when Coulomb screening is considered with a carrier density of 1×10^{12} cm^{-2}. There are three reasons why CH confinement is difficult:

(1) The mass of CH along the *c*-axis is very light (lighter than electron mass of GaN).
(2) Bandgap discontinuity between $Al_xGa_{1-x}N$ and $Al_yGa_{1-y}N$ is small when $x > 0.8$.
(3) AlGaN has a smaller VB-offset ratio (~0.2) compared to that of InGaN (~0.3), reducing the VB bandgap discontinuity.[17]

Unfortunately, CH is extremely difficult to confine and we cannot find suitable properties, even if the Coulomb screening effect is considered. Thus, in the following we discuss only the case where HH is on top for *c*-plane QWs.

On the other hand, the order of the VB energies in the nonpolar case is independent of Al content, as illustrated in Fig. 1(b). In most cases, the energy splitting between the two topmost VBs (X' and Y') is large. Thus, we can consider the VB as single band for any Al content. The definitions of crystal coordinates and VB labels for the nonpolar plane are the same as that in Ref. 18, where x' and z' are parallel to the *c*-axis and growth direction, respectively, and y′ is perpendicular to the other two axes. The analytical eigenenergy of the VBs for the nonpolar case is also given in that article. Additionally, the large energy splitting makes VB parabolicity good and the top VB of the nonpolar plane has an optical matrix element only for $E \parallel c$ with the TE mode (x'-polarization) for any Al content. Furthermore, the *c*-axis of $Al_xGa_{1-x}N$ is compressively strained on $Al_yGa_{1-y}N$, and it helps increase the VB energy of X' as the Al content x increases.

In summary, Figs. 1(c)–1(e) show the possible Fabry–Pérot-type cavity geometry of *c*-plane $Al_xGa_{1-x}N$/AlN with low x, *c*-plane Al_xGa_{1-x}/AlN with high x, and nonpolar $Al_xGa_{1-x}N$/AlN. One advantage of nonpolar AlGaN, especially at high Al compositions, is the optical matrix elements are suitable for both LD and LED applications.

A. *c*-plane QWs

1. Overlap and transition energy of thin QWs on the c-plane

The QCSE reduces the optical transition probability of *c*-plane AlGaN QWs. Hence, we initially attempted to increase the overlap integral $|\langle\varphi_c|\varphi_v\rangle|^2$ maximum, where φ_c and φ_v are the fundamental eigenfunctions of the conduction band (electrons) and the top VB (holes), respectively. The idea is simple; reducing the quantum well width suppresses the QCSE. The emission has been successfully enhanced using this method.[2,7] Figure 2(a) shows the dependence of the overlap integrals of $Al_xGa_{1-x}N$/AlN with well width. The overlap exceeds 70% when well width is below 1.0 nm (~4 ML). It is worth describing how a thin well width gives such a high overlap, although the internal field is large (e.g., 5.5 MV/cm in GaN/AlN QWs). When $x = 0.8$, the overlap integral in wells thinner than 1 nm becomes smaller compared to those $x < 0.8$ because the bandgap discontinuity between the well and barrier is very small. Additionally, the overlap integral of $Al_{0.8}Ga_{0.2}N$ wells

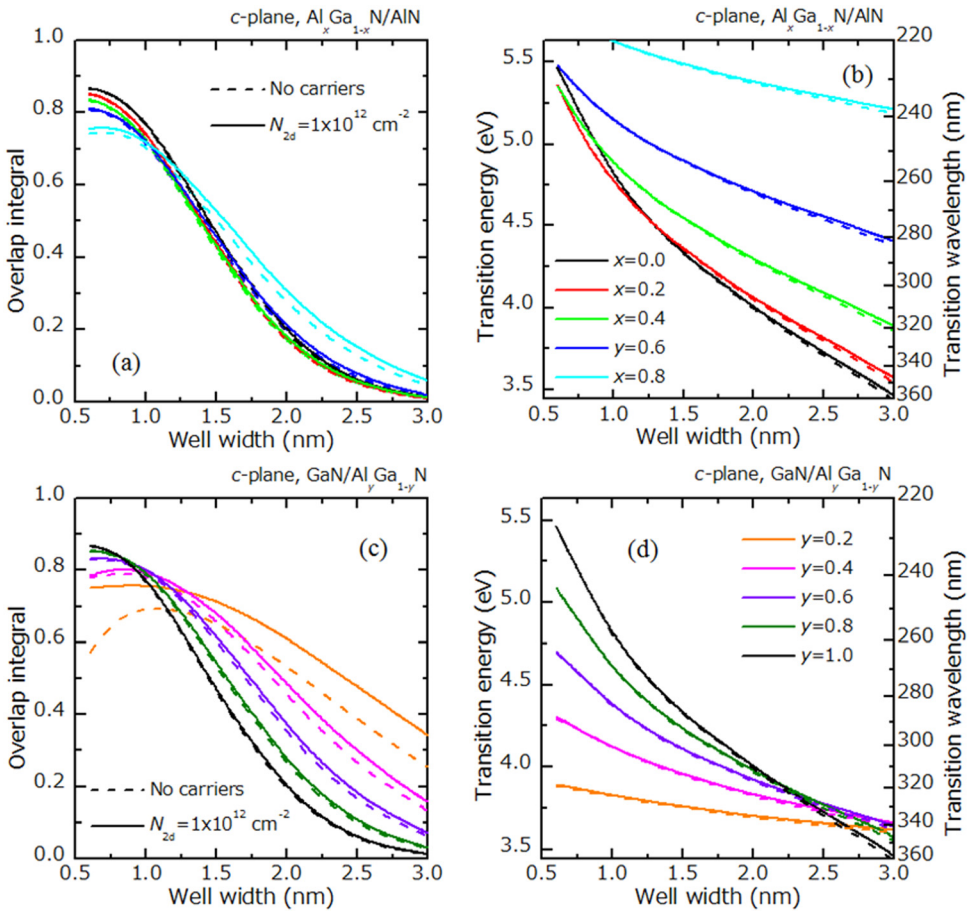

FIG. 2. (Color online) (a) Overlap integral of $Al_xGa_{1-x}N$/AlN QWs and (b) transition energy and wavelength of $Al_xGa_{1-x}N$/AlN QWs, (c) overlap integral of GaN/$Al_yGa_{1-y}N$ QWs, and (d) transition energy and wavelength of GaN/$Al_yGa_{1-y}N$ QWs. Crystal orientation is the *c*-plane. In experiments, well width becomes integral multiple of monolayer thickness of well material.

thicker than 1 nm becomes larger than that of $Al_xGa_{1-x}N$ QWs with $x < 0.8$ because the internal field decreases due to the lower strain of the well.

To reduce the QCSE, the well width should be narrow. However, a narrow well blueshifts the optical transition [Fig. 2(b)] due to the quantum effect. Even if the well material is GaN, the transition wavelength is nearly 260 nm when the well width is 1 nm. Thus, we investigated GaN/$Al_yGa_{1-y}N$ QWs. The well material GaN has the smallest bandgap among $Al_xGa_{1-x}N$, and lowering y can reduce both the confinement potential and hydrostatic energy shift, resulting in a reduced transition energy. The computed overlap and transition energy of GaN/$Al_yGa_{1-y}N$ QWs are illustrated in Figs. 2(c) and 2(d), respectively. In a GaN/$Al_yGa_{1-y}N$ QW system, a thin well width has large overlap, and ~330 nm can be achieved using $y = 0.2$, ensuring the overlap is more than 70% with a 1-nm-thick well. Although 345 nm is possible using a wider well with $y = 0.2$, the overlap is suppressed to about 30%. When the difference between *x* and *y* is small, the Coulomb screening effect by free carriers can slightly recover the overlap (Fig. 2), but the recovered overlap is not significant when the difference between *x* and *y* is large.

2. Threshold carrier density of c-plane QW lasers

Figure 3(a) shows the threshold carrier density as a function of well width for *c*-plane GaN/AlN QWs.[19] The threshold carrier density has a minimum near 1 nm. Wide QWs

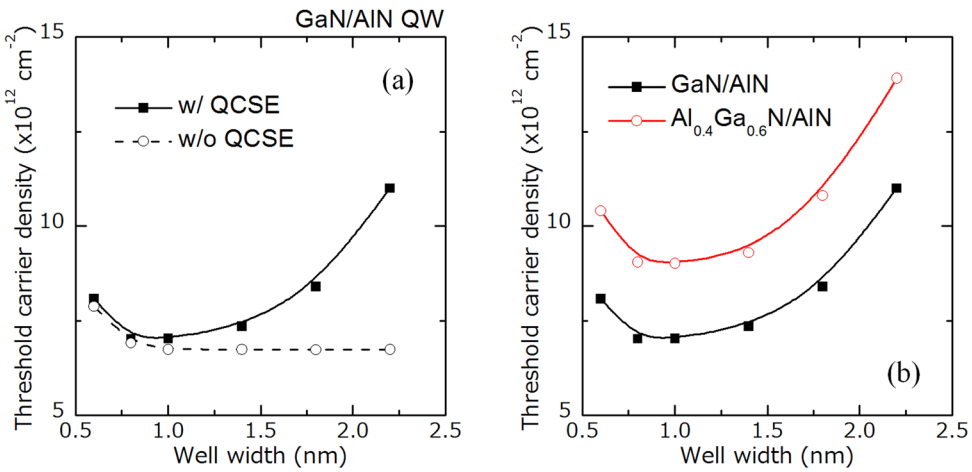

FIG. 3. (Color online) Well width dependence of the threshold carrier density of *c*-plane GaN/AlN QWs. (a) Threshold dependence on QCSE and (b) threshold dependence on Al content.

TABLE I. In-plane effective masses of *c*-plane QWs.

c-plane	m_c	m_{HH}
GaN	0.20	2.0
AlN	0.32	10

have larger thresholds due to the QCSE, because the internal field cannot be fully screened even under many carriers. A very small well width (<1 nm) rapidly increases the threshold. This degradation is due to the increased density of state of conduction band (CB) and VB caused by the wave function penetration to the barrier.[20] Ideally the density of state of the particles is determined only by the well material when the carrier envelopes localize in the well. However, carriers in a very narrow well partially overlap with the barrier layer, and the characteristics of the barrier material also affect the radiation process. Because electrons and holes of AlN are the heaviest among nitride semiconductors, heavy mass in a barrier induces a large density of state for active layers sandwiched by an AlN or Al-rich AlGaN barrier. As discussed in the previous section, a smaller overlap integral decreases the optical gain, but its contribution is minor in the rapid increase of the threshold in a narrow well.

Figure 3(b) depicts the threshold carrier density as a function of well width for GaN/AlN and $Al_{0.4}Ga_{0.6}N$/AlN single QWs. $Al_{0.4}Ga_{0.6}N$ QWs have larger thresholds compared to GaN QWs, although both have similar overlap integrals [Fig. 2(b)]. The threshold of the $Al_{0.4}Ga_{0.6}N$ QW on the *c*-plane is high mainly due to the heavy mass. Table I; shows the in-plane effective masses of both electrons and holes (HH). HH of AlN is five times larger than that of GaN. Because population inversion requires the probability of both electrons and holes to be excited, a heavy mass requires a higher excitation to achieve inversion. Therefore, the Al content of the well material should be reduced.

B. Nonpolar plane QWs

1. VB energy diagram

Figures 4(a) and 4(b) represent the VB energy structure of nonpolar GaN/$Al_yGa_{1-y}N$ and $Al_xGa_{1-x}N$/AlN, respectively. When $y = 0$ in GaN/$Al_yGa_{1-y}N$, the emitter material is simply unstrained GaN. Thus, we labeled the three VBs using HH, light hole (LH), and CH as indicated in the inset of Fig. 4(a). When $y \neq 0$, VBs are mixed due to anisotropic strain and the three VBs should be relabeled using their polarization and the method reported in Ref. 18. When *y* is less than 0.15, the top VB is *Y'*, but it becomes *X'* for $y > 0.15$ 0 [inset of Fig. 4(a)]. If the deformation potentials in Ref. 15 are adopted, then the singular *y* value changes from 0.15 to 0.30. Details are discussed elsewhere.[21] On the other hand, band *X'* is the top VB of $Al_xGa_{1-x}N$/AlN [Fig. 4(b)], regardless of the value of *x* and is independent of the variation in the deformation potential due to the large negative value of Δ_{cr} and the compressively strained c-axis. The top VB becomes CH when $x = 1.0$ where the emitter material represents unstrained AlN bulk. It is noteworthy that the top VBs of GaN/$Al_yGa_{1-y}N$ with a large *y* and $Al_xGa_{1-x}N$/AlN are energetically isolated from other VBs; consequently, the optical polarization between CB and the top VB is almost unity and most of the holes populate only the top VB even at room temperature. This characteristic is ideal for LD applications.

2. Overlap integral and transition energy between CB and the top VB of nonpolar QWs

Figures 5(a) and 5(b) show the overlap integral and transition energy of GaN/$Al_yGa_{1-y}N$ QWs with quantum well thickness, respectively. Due to the absence of the QCSE, the well width can be thicker for nonpolar QWs, which nicely confines carriers more than 0.9, even for GaN/$Al_{0.2}Ga_{0.8}N$ where the bandgap discontinuity is relatively small. This is a critical advantage of the nonpolar plane. As discussed earlier, the VB offset ratio of AlGaN is small and carrier confinement in GaN/$Al_yGa_{1-y}N$ with low y is difficult. Similarly, $Al_xGa_{1-x}N$/AlN QWs have large overlap integral values, even with a high Al content *x*. Figures 5(c) and 5(d) show the overlap integral and transition energy of $Al_xGa_{1-x}N$/AlN QWs, respectively.

Even when the top VB of GaN/$Al_yGa_{1-y}N$ becomes *Y'* by decreasing Al content *y* as shown in Fig. 4(a), the confinement properties of the holes are nearly independent of *y* because the vertical masses of *X'* and *Y'* (incidentally, HH) are close to each other.18 Furthermore, both VB *X'* and *Y'*

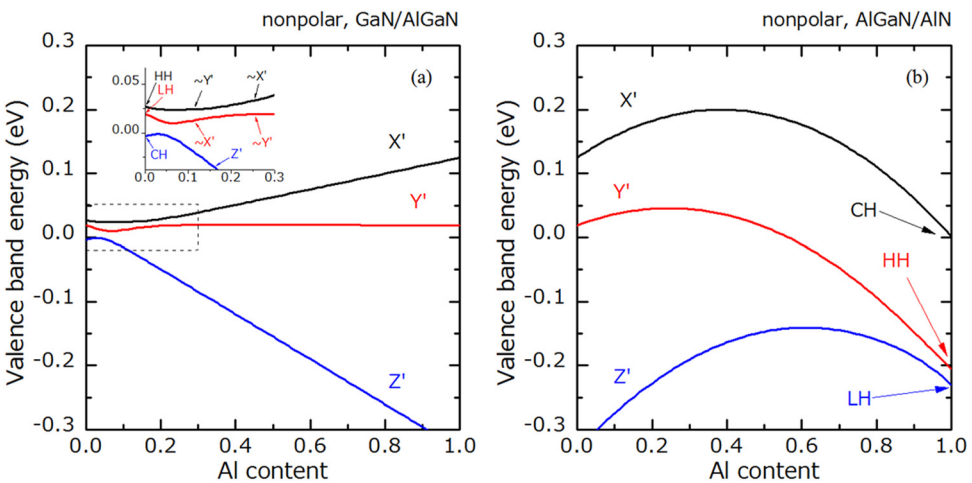

FIG. 4. (Color online) VB energy structure of (a) nonpolar GaN/$Al_yGa_{1-y}N$ and (b) nonpolar $Al_xGa_{1-x}N$/AlN strained bulks. Origin of VB energy is set to the VB energy of an unstrained bulk crystal without crystal-field splitting and spin-orbit interaction. Inset in (a) magnifies the VB structure with an Al content from 0.0 to 0.3.

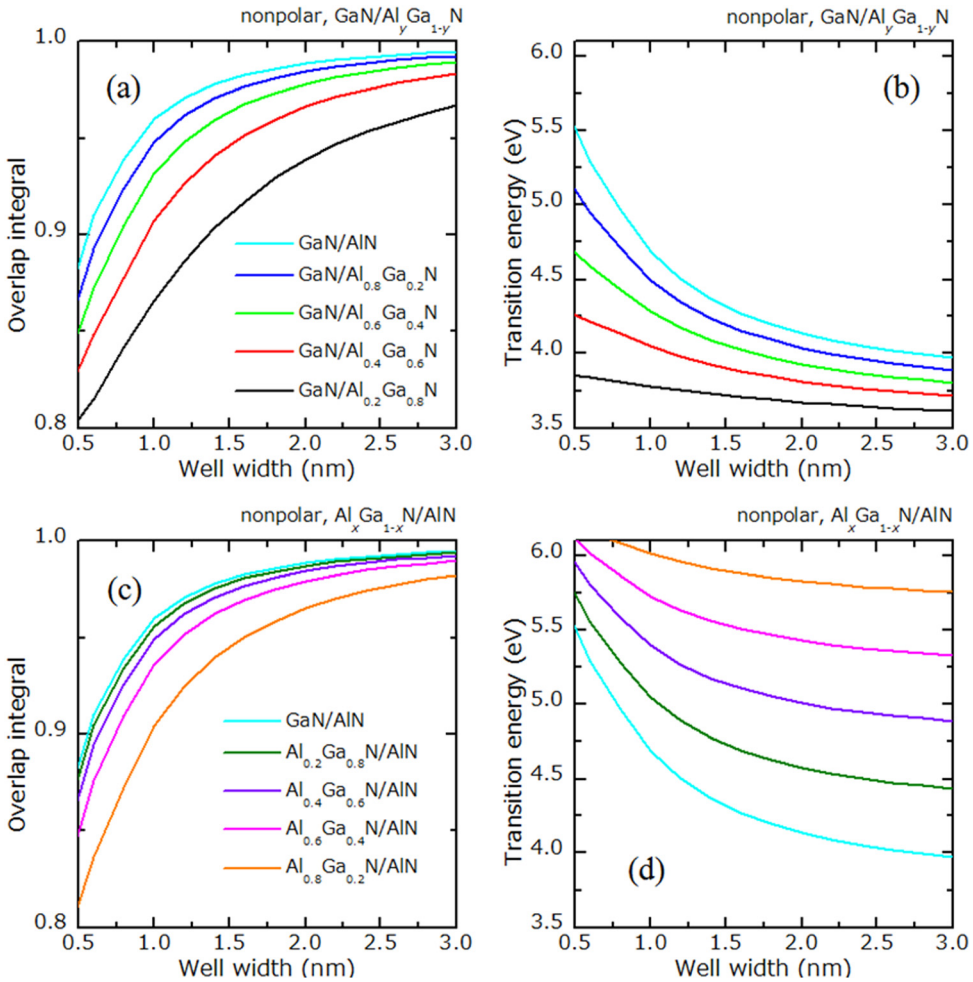

FIG. 5. (Color online) (a) Overlap integral of GaN/Al$_y$Ga$_{1-y}$N QWs, (b) transition energy of GaN/Al$_y$Ga$_{1-y}$N QWs, (c) overlap integral of Al$_x$Ga$_{1-x}$N/AlN QWs, and (d) transition energy of Al$_x$Ga$_{1-x}$N/AlN QWs. Crystal orientation is the nonpolar plane.

can contribute to the surface emission. Thus, the wavelength range of an AlGaN emitter as a LED can be controlled between the bandgap of GaN and AlN while maintaining a high overlap.

3. Optical gain of nonpolar QWs

Figures 6(a) and 6(b) represent the anisotropic optical gain of nonpolar and *c*-plane 1-nm-thick GaN/AlN single QWs, respectively. For comparison, the well widths are fixed to 1 nm, which is the optimized condition for the *c*-plane. Because the top VB of nonpolar GaN/AlN is X', $E \parallel c$ polarization dominates gain formation. Furthermore, the energy separation between the top VB and the second VB of this system is large (Fig. 4). Hence, the carrier population is distributed almost exclusively in the top VB, which assists gain formation. The very weak gain obtained with $E \perp c$ (in-plane, y') also relates the top VB possessing some wave number, and not the second VB.

Figures 6(a) and 6(b) clearly show that the gain of a nonpolar QW is superior to that of a *c*-plane QW due to (1) the absence of the QCSE, (2) polarization matrix elements,

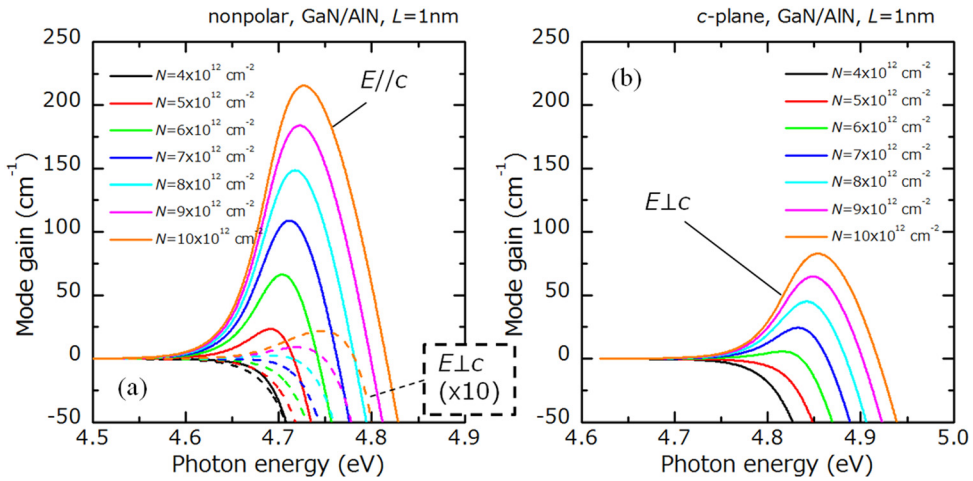

FIG. 6. (Color online) Optical gain of 1-nm-thick AlGaN QWs on the (a) nonpolar plane and (b) *c*-plane.

and (3) the reduction of density of state. As previously mentioned, because a thin well can reduce QCSE in *c*-plane QWs, the first point has a relatively minor contribution in the gain formation difference. With regard to the polarization matrix elements, the optical matrix element is isotropically distributed on the *c*-plane, but is focused in the x' direction on the nonpolar plane. Thus, the matrix element of nonpolar QWs is twice that of the *c*-plane, which greatly improves the gain. Although the reduced density of states has been documented elsewhere[12,22] and investigated quantitatively,[18] we stress that it is the most critical issue to realize high-performance DUV emitters.

AlN has the heaviest mass among InN, GaN, and AlN, and the density of state is also the highest. The trend where lighter constituent atoms induce a heavier effective mass is also found in other semiconductors like GaAs and GaP families and is related to the atomic number of V materials. Thus, the threshold of AlGaN LDs potentially becomes higher as the Al content increases.

Let us estimate how the nonpolar orientation can reduce the VB effective mass of AlGaN. Table II shows the effective masses of CB (electron) and VB (holes) with an X' base by using the analytical solution in Ref. 18. The effective masses of AlGaN can be roughly estimated from Table II by interpolation. Note that native binaries should have effective masses of mHH or mCH, but Table II is still useful to understand how the nonpolar $Al_xGa_{1-x}N/Al_yGa_{1-y}N$ orientation can reduce VB mass. Comparing Tables I and II we can evaluate how the nonpolar orientation reduces the in-plane mass for the extreme cases of GaN and AlN. The VB mass reduction ratio $\sqrt{m_2^{x'}m_2^{y'}}/m_{\mathrm{HH}}^{\perp}$ is 10% in the AlN case, which is small compared to that of GaN (28%) or InN (30%). This fact implies the nonpolar orientation can greatly improve the performance of AlGaN LDs, and compared to an InGaN system should more effectively improve the performance. The difference in the VB mass reduction ratio between AlN and GaN or InN is due to the base difference.

IV. COMPARISON OF *C*-PLANE AND NONPOLAR LASERS

Figure 7 shows the maximum gain of 1-nm-thick GaN/AlN QWs on the *c*-plane and nonpolar plane. The gain properties for both the transparent carrier density and differential gain of nonpolar QWs are superior to those for the *c*-plane ones due to the reasons discussed earlier. Hence, it is predicted that nonpolar QWs can maintain a lower threshold carrier density compared to the *c*-plane case, even when light confinement is low and/or internal loss increases upon increasing the Al content in both the active and cladding layers.

TABLE II. In-plane effective masses of nonpolar plane QWs.

Nonpolar	m_c	$\sqrt{m_2^{x'}m_2^{y'}}$	VB mass reduction ratio (nonpolar/*c*-plane) (%)
GaN	0.20	0.56	28
AlN	0.32	1.0	10

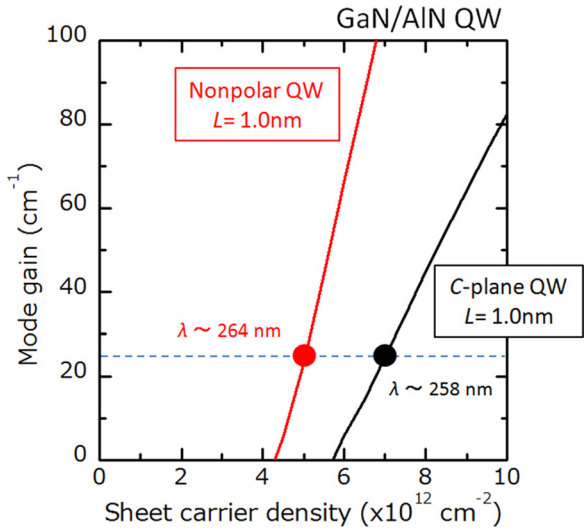

FIG. 7. (Color online) Comparison of threshold carrier density between nonpolar and *c*-plane GaN/AlN QWs with well widths of 1 nm.

Figure 8 shows the threshold carrier density of 1-nm-thick nonpolar and *c*-plane $Al_xGa_{1-x}N/Al_yGa_{1-y}N$ QWs as functions of their transition wavelengths. The threshold of nonpolar QWs is smaller than that of the *c*-plane QWs in a wavelength range between 200 and 340 nm. For $GaN/Al_yGa_{1-y}N$ with low y, the threshold of nonpolar QWs with $E\perp c$ (y'-polarization) is less than that of $E \parallel c$ (x'-polarization) due to the anticrossing of VBs of X' and Y' as pointed out in Fig. 4(a). The top VB can change between X' and Y', however, the threshold of nonpolar QWs is equal to or less than that of the *c*-plane one. Furthermore, both X' and Y' provide TE-mode gain. Therefore, the cavity direction should be carefully considered.

The most important point in Fig. 8 is the huge threshold difference in the wavelength regime shorter than 260 nm. In

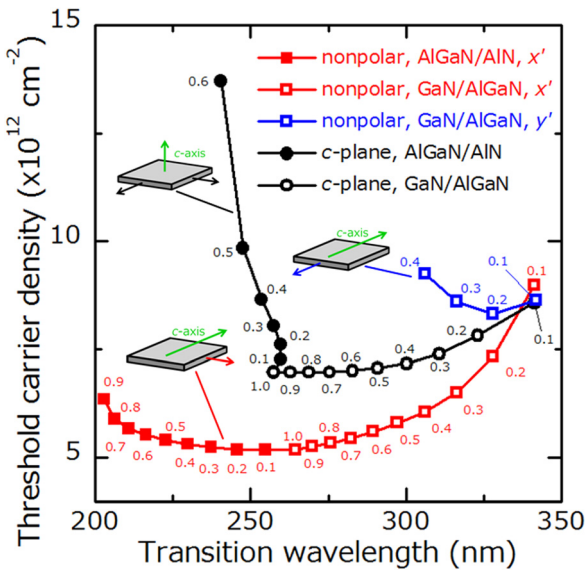

FIG. 8. (Color online) Threshold carrier density of 1-nm-thick $Al_xGa_{1-x}N/Al_yGa_{1-y}N$ QWs. Black, red, and blue lines represent the threshold for *c*-plane QWs, nonpolar QWs with $E \parallel c$ (x'-polarization), and nonpolar QWs with $E\perp c$ (y'-polarization), respectively. Small numbers indicate Al content.

this regime, the well Al content x is greater than zero and density of state of VB increases with increasing x. However, the VB effective mass of nonpolar QWs is relatively small, whereas that of the c-plane is enormous. Thus, the threshold of nonpolar LDs remains small, even for a high Al content x. In contrast, the threshold drastically increases for a c-plane LD with a high Al context x. Moreover, when x of the c-plane $Al_xGa_{1-x}N$ QW increases, CH approaches HH. Consequently, the carrier population is distributed for both VBs, resulting in a gain partition for both the TE and TM modes. This also pushes the threshold up. Nonpolar QWs can also accept a wide well width, which should be less than the critical thickness. Hence, widening the well should extend the low threshold regime.

V. SUMMARY

We theoretically compared the radiation properties of nonpolar AlGaN QWs and c-plane AlGaN QWs. We initially examined c-plane QWs with HH as the top VB. A thin well width around 1 nm is ideal to minimize the threshold carrier density. Additionally, reducing the Al content in the well layer is important because a narrow well suppresses QCSE and simultaneously increases overlap. Moreover, AlGaN with a lower Al content has a smaller density of states.

Next, we investigated the VB energy structure, overlap integral, transition energy, and optical gain of nonpolar AlGaN QWs. Compared to c-plane QWs, nonpolar AlGaN has several superior characteristics, including large overlap integrals, suitable polarization for both edge and surface emissions (X' or Y'), a nearly linearly polarized optical dipole between CB and the top VB, and a reduction in the VB density of state. Consequently, nonpolar QWs have a lower transparent carrier density and higher differential gain. Thus, nonpolar QWs should possess a lower threshold carrier density compared to the c-plane case.

Finally, we compared the threshold carrier densities of both nonpolar and the optimized c-plane QWs as functions of the transition wavelength. Regardless of wavelength, the threshold of nonpolar QWs is less than that of c-plane ones, especially below 260 nm where nonpolar QWs maintain a low threshold, but the threshold of the c-plane QWs drastically increases.

ACKNOWLEDGMENTS

This work was supported by KAKENHI (21016006).

[1]Y. Taniyasu, M. Kasu, and T. Makimoto, Nature (London) **441**, 325 (2006).
[2]H. Hirayama, N. Noguchi, and N. Kamata, Appl. Phys. Express **3**, 032102 (2010).
[3]M. A. Khan, M. Shatalov, H. P. Maruska, H. M. Wang, and E. Kuokstis, Jpn. J. Appl. Phys. **44**, 7191 (2005).
[4]T. Oto, R. G. Banal, K. Kataoka, M. Funato, and Y. Kawakami, Nat. Photonics **4**, 767 (2010).
[5]K. B. Nam, J. Li, M. L. Nakarmi, J. Y. Lin, and H. X. Jiang, Appl. Phys. Lett. **84**, 5264 (2004).
[6]H. Kawanishi, M. Senuma, and T. Nukui, Appl. Phys. Lett. **89**, 041126 (2006).
[7]R. G. Banal, M. Funato, and Y. Kawakami, Phys. Rev. B **79**, 121308(R) (2009).
[8]H. Yoshida, Y. Yamashita, M. Kuwabara, and H. Kan, Nat. Photonics **2**, 551 (2008).
[9]M. Horita, T. Kimoto, and J. Suda, Appl. Phys. Express **3**, 051001 (2010).
[10]A. A. Yamaguchi, Appl. Phys. Lett. **96**, 151911 (2010).
[11]S. L. Chuang and C. S. Chang, Phys. Rev. B **54**, 2491 (1996).
[12]S. H. Park and S. L. Chuang, Phys. Rev. B **59**, 4725 (1999).
[13]S. Wei and A. Zunger, Appl. Phys. Lett. **69**, 2719 (1999).
[14]I. Vurgaftman and J. R. Meyer, J. Appl. Phys. **94**, 3675 (2003).
[15]R. Ishii, A. Kaneta, M. Funato, Y. Kawakami, and A. A. Yamaguchi, Phys. Rev. B **81**, 155202 (2010).
[16]A. A. Yamaguchi, Phys. Status Solidi C **5**, 2364 (2008).
[17]G. Martin, A. Botchkarev, A. Rockett, and H. Morkoç, Appl. Phys. Lett. **68**, 2541 (1996).
[18]K. Kojima, M. Funato, Y. Kawakami, and S. Noda, *J. Appl. Phys.* **107**, 123105 (2010).
[19]Optical confinement factor Γ was evaluated by, $\Gamma = 0.0053 L_w$ (nm) and internal loss was assumed to be 25 cm^{-1} to calculate modal gain. These values are assumed by considering a typical nitride QW LD structure.
[20]A. Sugiyama, IEEE J. Quantum Electron. **19**, 932 (1983).
[21]R. Ishii, A. Kaneta, M. Funato, and Y. Kawakami, Jpn. J. Appl. Phys. **49** 060201 (2010).
[22]T. Ohtoshi, A. Niwa, and T. Kuroda, *Jpn. J. Appl. Phys.* **35**, L1566 (1996).